Isotopic quantum effects in the structure of liquid methanol: I. Experiments with high-energy photon diffraction

2001 J. Phys.: Condens. Matter 13 11405

(http://iopscience.iop.org/0953-8984/13/50/301)

INSTITUTE OF PHYSICS PUBLISHING JOURNAL OF PHYSICS: CONDENSED MATTER

J. Phys.: Condens. Matter **13** (2001) 11405–11420 PII: S0953-8984(01)29583-6

Isotopic quantum effects in the structure of liquid methanol: I. Experiments with high-energy photon diffraction

B Tomberli[1], P A Egelstaff[1], C J Benmore[2,3] and J Neuefeind[4]

[1] Department of Physics, University of Guelph, Guelph, Ontario, Canada N1G 2W1
[2] IPNS Division, Argonne National Laboratory, 9700 S. Cass Ave., Argonne, IL 60439, USA
[3] ISIS Facility, CLRC Rutherford Appleton Laboratory, Chilton, Oxon OX11 OXQ, UK
[4] Hamburger Synchrotronstrahlungslaboratorium HASYLAB at Deutsches Elektronensynchrotron DESY, Notkestr. 85, 22603 Hamburg, Germany

Received 10 October 2001
Published 30 November 2001
Online at stacks.iop.org/JPhysCM/13/11405

Abstract

High-energy electromagnetic radiation scattering techniques have been used to measure the structural differences between four isotopic samples of methanol (CH_3OH, CD_3OD, CH_3OD and CD_3OH). The first series of experiments employed room temperature and ambient pressure. The carbon–oxygen intramolecular bond length was measured and found to depend more strongly on the isotopic substitution at the hydroxyl site than at the methyl sites. The oscillations in the isotopic difference of the x-ray structure factor, $\Delta S_X(Q)$, are shown at room temperature to be about 2% as large as the oscillations in the total structure factor. Our uncertainties are an order of magnitude smaller than those of previous gamma ray measurements (Benmore C J and Egelstaff P A 1996 *J. Phys.: Condens. Matter* **8** 9429–32). A second series of experiments was carried out at −80 °C at its vapour pressure in order to study the significant temperature dependence of these effects. The $\Delta S_X(Q)$ difference at −80 °C is shown to be up to three times larger than the room temperature difference. These studies showed that isotopic structural differences in methanol may be represented as temperature shifts that vary as a function of thermodynamic state and substitution site.

(Some figures in this article are in colour only in the electronic version)

1. Introduction

While quantum effects in molecular liquids are well documented at low temperatures, at room temperature samples are assumed in many cases to be comprised of molecules that behave classically. The validity of such simplifications for hydrogenous liquids is challenged by the fact that their bulk properties show isotopic variations (e.g. water[5]). Some of these effects

[5] Melting points 0.00 °C for H_2O and 3.82 °C for D_2O. Boiling points 100.00 °C for H_2O and 101.42 °C for D_2O. These values were taken from [2].

clearly have a quantum mechanical origin: for example, a classical simulation using the same potential for two different isotopes would obtain the same structure for all isotopic molecular liquids of a particular compound, whereas a quantum simulation does not [3]. Therefore, for the interpretation of accurate experimental structural results on hydrogenous molecular liquids, quantum corrections to the classical assumptions are required even at room temperature [1].

We have used synchrotron radiation at ESRF and HASYLAB to measure directly and accurately the differences, $\Delta S_x(Q)$, in the static structure factors for methanol before and after H to D substitutions at varying sites. Although the isotopes have a different mass, the atoms have essentially the same electronic structure, therefore any isotopic difference measured in the molecular structure factor $\Delta S_x(Q)$ will be due to quantum-induced differences. The effect in both the intra- and intermolecular liquid structure has been measured accurately by these isotopic differences between the electronic structure factors.

In the past, results from several experiments on the classical x-ray structure of methanol have been published in the literature [4–6]. However, the quantum effect in methanol was first observed experimentally by the low-intensity γ-ray experiments of Benmore and Egelstaff [1]. Although they were successful in measuring a small isotopic effect upon the fluid structure, the accuracy of their work was limited by statistical errors. With the advent of powerful synchrotron sources, such measurements can be improved substantially and thus more precise experiments have become possible.

We note that for room temperature liquids, quantum isotopic effects force quantities such as the intramolecular distances and the bulk number densities of liquids containing different isotopes to differ slightly. Previously published results on water [7]—for which the isotopic dependence of the number densities and intramolecular structure are available—have shown that these isotopic effects lead to intermolecular effects much smaller than the measured $\Delta S_x(Q)$ for water. Thus detailed isotopic structural effects were observed experimentally in scattering experiments on water [7]. We have followed the same procedures in these experiments on liquid methanol.

In order to obtain high-quality electromagnetic radiation scattering measurements, we shall measure the intra- and intermolecular structure for various isotopic samples of methanol using high-intensity beams of (approx.) 110 keV synchrotron radiation together with low angles of scatter. Moreover, the results of such isotopic difference measurements could be useful in the evaluation of corrections to neutron diffraction hydrogen–deuterium substitution experiments, wherein the difference in the intermolecular structure between isotopic samples is usually assumed to be zero (e.g. [8]). We note that this assumption has been used in recent work on alcohols [9, 10].

Our experiments should also provide a better test of the intermolecular potentials used in quantum mechanical calculations for methanol. Methanol is believed to form hydrogen-bonded chains in the liquid [4–7]. It is expected that substantive corrections to the classical model of molecular interactions could be caused by the coupling of intra and inter modes by hydrogen bonding, by differences in their ground state librations, and by many-body effects. Such phenomena generate differences between the structures of the H and D molecular liquids. Thus, agreement of a particular model with our measured results would support its use in estimating all these effects. It would also be useful to examine the differences between our observations and the quantum mechanical predictions to study the general assumptions made in deriving the potential using quantum mechanics. At the present time specific examples are not available for methanol. In a wider context there may be applications of these data in the fields of chemistry, medicine and engineering where sophisticated applications of H/D compounds might be employed and studied.

In this paper we describe the experiments and the reduction of the results to the static structure factor, $S(Q)$. The transformation of the data to r-space (which emphasizes the intramolecular properties) will be discussed in paper II. However, some examples of these experiments have been reported in a letter [11].

2. Theoretical development

A brief synopsis of the methods used is presented here. Details of the theory involved in this diffraction experiment are available in a previously published work on water [7] as well as in standard reference texts (e.g. [12, 13]).

The atom–atom partial pair distribution functions, $g_{\alpha\beta}(r)$, for a molecular fluid are related to the intermolecular partial site–site structure factors $D_{\alpha\beta}(Q)$ through Fourier transform relations: for example,

$$D_{\alpha\beta}(Q) = \rho \int \mathrm{d}r \, \exp(\mathrm{i}Q \cdot r)[g_{\alpha\beta}(r) - 1] \tag{1}$$

where α and β denote particular atoms, ρ is the molecular density and Q is the momentum transfer [13]. Using the approximation that each atom scatters radiation independently, an electromagnetic diffraction experiment observes the following weighted sum of the $D_{\alpha\beta}(Q)$ [4] for methanol:

$$\begin{aligned} D_X(Q) = {} & f_{\mathrm{O}}^2(q)D_{\mathrm{OO}}(Q) + f_{\mathrm{C}}^2(q)D_{\mathrm{CC}}(Q) + 2f_{\mathrm{O}}(q)f_{\mathrm{C}}(q)D_{\mathrm{OC}}(Q) \\ & + 8f_{\mathrm{O}}(Q)f_{\mathrm{H}}(Q)D_{\mathrm{OH}}(Q) + 8f_{\mathrm{C}}(Q)f_{\mathrm{H}}(Q)D_{\mathrm{CH}}(Q) + 16f_{\mathrm{H}}^2(q)D_{\mathrm{HH}}(Q) \end{aligned} \tag{2}$$

where the f_α are the Q-dependent atomic form factors, tabulated in the literature [14]. $D_X(Q)$ is related to the structure factor, $S_X(Q)$, by the equation

$$D_X(Q) = S_X(Q) - \langle F^2 \rangle \tag{3a}$$

where $\langle F^2 \rangle$ is the intramolecular scattering function. Furthermore, the structure factor, $S_X(Q)$, can be calculated from $I_X(Q)$ (see section 4), the intensity measured in a diffraction experiment, and the known Compton scattering $C_X(Q)$ [14]:

$$S_X(Q) = I_X(Q) - C_X(Q). \tag{3b}$$

The quantity $\langle F^2 \rangle$ depends on the intramolecular structure and is approximately that for isolated single molecules. It can be estimated using the independent atom approximation (IAA) [4]. We will show in section 4 that the accuracy of IAA in determining $\langle F^2 \rangle$ at high Q-values where it is used to normalize the experimental data is sufficient for our purposes.

For a molecule of known structure, the intramolecular scattering $\langle F^2 \rangle$ approximated by the IAA is given by

$$\langle F^2 \rangle = \sum_i \sum_j f_i f_j \frac{\sin r_{ij}Q}{r_{ij}Q} \exp(-b_{ij}Q^2). \tag{4}$$

The summation is over all scattering centres in the molecule, each with spatial separation r_{ij} and positional variances b_{ij}. Literature estimates of the intramolecular structure of methanol samples in various states are tabulated in table 1. Later, we will use our experimental data to determine the value of r_{CO} for each isotope and compare our values to those in table 1.

$C_X(Q)$ in equation (3) is the Compton scattering which can be found by summing the atomic contributions which are tabulated in the literature. As Q increases, $C_X(Q)$ asymptotically approaches the number of electrons, with relativistic corrections as given by the Klein–Nishina formula. As will be seen in section 4, this quantity can be used to normalize $I_X(Q)$ in units of electrons per molecule. The error in $S_X(Q)$ caused by approximating $C_X(Q)$

Table 1. Structural parameters from the literature for methanol isotopic samples.

	CH_3OH	CD_3OH	CH_3OD	CD_3OD
r_{CO} (Å)	1.437 ± 0.002 [4]	1.425 ± 0.002 [6]	1.425 ± 0.002 [6]	1.418 ± 0.01 [15]
r_{OH_1} (Å)	0.9451 ± 0.003 [16]	0.9451 ± 0.003 [16]	1.030 ± 0.01 [15]	1.030 ± 0.01 [15]
r_{CH_3} (Å)	1.0936 ± 0.003 [16]	1.066 ± 0.003 [15]	1.0936 ± 0.003 [16]	1.066 ± 0.003 [15]
∠COH1	108.5° ± 0.5° [16]	108.5° ± 0.5° [16]	101.6° ± 1.5° [15]	101.6° ± 1.5° [15]
Methyl tilt	3.25° ± 0.2° [16]	3.25° ± 0.2° [16]	3.25° ± 0.2° [16]	3.25° ± 0.2° [16]
b_{CO} (Å^2)	0.0012 ± 0.001 [17]	0.0012 ± 001 [17]	0.0012 ± 001 [17]	0.0012 ± 001 [17]
b_{OH_1} (Å^2)	0.0025 ± 0.006 [17]	0.0027 ± 0.006 [17]	0.0015 ± 0.0003 [15][a]	0.0015 ± 0.0003 [15][a]
b_{CH_3} (Å^2)	0.0032 ± 0.0004 [17]	0.0024 ± 0.0003 [15][b]	0.0032 ± 0.0004 [17]	0.0024 ± 0.0003 [15]

[a] Average of 0.5 and 0.7 Å data from [15].
[b] Chose 0.7 Å value from [15] for better agreement with expected value = (protonated values)/$\sqrt{2}$.

by the sum of the atomic contributions is similar to that introduced by using the IAA for $\langle F^2 \rangle$. In section 4 we show that this error is much smaller than our statistical error bars. Finally the pseudonuclear scattering function per molecule, $i(Q)$, is obtained from the equation

$$i\,(Q) = \frac{S_X\,(Q) - \sum_i f_i^2\,(Q)}{(\sum_i f_i\,(Q))^2} \tag{5}$$

where f_i is the form factor for atom i. This function can be transformed to yield a molecular pseudonuclear correlation function in r-space:

$$g_X(r) = 1 + \frac{1}{2\pi^2 \rho r} \int Q\, i(Q)\, \sin(Qr)\, \mathrm{d}Q \tag{6}$$

where ρ is the molecular density per Å^3. The X subscript indicates that the electronic structure factor was used to derive the correlation function. The difference between measurements on H and D compounds will be denoted by $\Delta g_x(r)$ and from (6) we see that $\Delta g_x(r) \to 0$ as $r \to 0$.

Therefore, accurate EM radiation scattering experiments are sensitive to any small isotopic differences in the intermolecular structure, and consequently they can set a limit upon the structural variations occurring through isotopic substitution in molecular fluids at our experimental temperatures.

3. Experimental details

The experiments were conducted on the diffractometer on the BW5 wiggler beamline on the DORIS III storage ring at DESY in Hamburg, Germany, and on an apparatus we constructed on the ID15A beamline at ESRF in Grenoble, France. During these experiments, measurements were made on water and compared with our previous work [7] in order to confirm that these experiments had achieved the accuracy required. The experimental procedure used at ESRF was exactly the same as that used for the previously published water measurements [7]. For the HASYLAB measurements the method was almost the same, and the minor differences are discussed in the summary of the methods given below.

Diagrams of the experimental set-ups (relevant lengths, beam dimensions etc) are provided in a recent publication [7]. Table 2 gives other information about the experiments: unless stated otherwise, all quantities have an uncertainty of ±1 in the last digit.

To reduce vessel scattering, all experiments used thin-walled (10 μm) silica tubes of 2–3 mm diameter to hold the liquid. Isotopically pure (99.99%+) methanol samples with chemical purities of CH_3OH (99.94% pure, 0.0004% H_2O), CD_3OD (99.91% pure, 0.0000% H_2O), CH_3OD (99.85% pure, 0.0000% H_2O) and CD_3OH (99.87% pure, 0.05% H_2O) were

Table 2. Experimental summary.

Data	ESRF–ID15A	HASYLAB–BW5	
Experiment date	July 1998	Sept. 1999	Sept. 2000
Temperature (°C)	23.5 ± 0.25	-80.6, 25.3	-80.0, -30.0, 24.5, 34.0[a]
Beam energy (keV)	116.2	100.0	100.0
Wavelength (Å)	0.1068	0.1241	0.1241
Horizontal polarization	90%	91%	91%
Q range (Å^{-1})	0.49–20.2	0.58–17.6	0.45–21.93
Deadtime (μs)	3.4	2.51	1.3

[a] These temperatures have an error ± 0.01 °C associated with them.

used. The samples were sealed in silica tubes which were fixed rigidly onto a translation table which sequentially centred each sample tube on the beam.

At HASYLAB the sample vessels were held in a 0.500 m diameter evacuated cylinder. Recent improvements (during 2000) to the BW5 diffractometer included the addition of a beam stop inside this cylinder to reduce multiple scattering in the cylinder and to screen out the incident beam. This allowed lower scattering angles to be studied than was possible in our previous experiments. The sample plus vessel, empty vessel scattering and background data were collected in a series of runs. The intensity incident on the sample was monitored accurately using a photodiode to correct for variations in the beam current at both ESRF and HASYLAB. This and other time-dependent effects were further reduced by interleaving many scans on each isotope.

Finally, the measured intensity in both experiments was corrected for detector deadtime (see table 2) and beam polarization. Also the nominal angles of scatter were corrected to the true angles from calibrations using aluminium Bragg peaks [7]. The HASYLAB data required a small additional geometric correction [7].

A maximum statistical variation of less than 0.5% in the region of the main peak for CH_3OH was observed between scans of the same sample in the same tube at ESRF. Averaging over the 12 scans taken for each isotope resulted in a total statistical error of 0.1%. A similar analysis of the HASYLAB results yields a mean statistical error of 0.4%.

4. Data reduction

It has been shown elsewhere [11, 18] that the quantity $I_X(Q)$ in equation (3*b*) is given by the following expression, where S indicates sample and V indicates its vessel;

$$I_X(Q) = K\left(\frac{I_0^{SV} - B}{A_{S,SV}} - \frac{A_{V,SV}\left(I_0^V - B\right)}{A_{S,SV}A_{V,V}}\right) - \frac{\sigma_{SV}}{4\pi b^2}M_{SV}. \tag{7}$$

Here I_0^{SV} and I_0^V are count rates from the sample plus vessel and empty vessel systems, respectively, after they were corrected for beam intensity, polarization, geometric effects, angle of scatter and dead time. B is the stray background count rate measured with the beam on but no sample or vessel in its path. M_{SV} is the multiple scattering estimate from the sample plus vessel [19], σ_{SV} is the scattering cross section for the sample plus vessel system [19] and $A_{i,jk}$ is a self-absorption factor for scattering in body i, and absorption in bodies j and k [20]. For photon scattering the isotopic differences in these quantities have been estimated and are negligible.

The classical radius for an electron is given by b, and K is the calibration constant to be determined individually for each sample plus tube system. This constant is found by using the fact that for our samples, $D_X(Q)/S_X(Q) < 0.001$ for $Q > 10$ Å^{-1}. Therefore we may find the constant K from equation (3b), where $I_X(Q) \cong \langle F^2 \rangle + C_X(Q)$ for $Q > 10$ Å^{-1}. $\langle F^2 \rangle$ may be calculated with sufficient accuracy by using equation (4) (the IAA) and $C_X(Q)$ from the Klein–Nishina formula. Such use of the IAA to normalize $S_X(Q)$ is reasonable because we use it only at high Q, where it is very good, in order to estimate the structure factor of each isotope there. The error introduced into $S_X(Q)$ by completely omitting the contribution of intramolecular structure during normalization was found to be about one part in 10^4. The small size of this error is due to the cancellation of the effects of the intramolecular structure over the normalization range. Therefore, by estimating intramolecular contributions using the IAA, the normalization error is further reduced. The use of a more sophisticated model to predict $\langle F^2 \rangle$ and $C_X(Q)$ more accurately is therefore not justified for the purposes of normalizing $S_X(Q)$. $S_X(Q)$ can thus be determined in absolute electron units for all isotopes over the entire measured range.

The isotopic difference $\Delta S_X(Q)$ at $Q = 0$, was set to zero for each isotopic difference since the differences in compressibility were not known and were expected to be small. The $\Delta S_X(Q)$ difference was extended from the lowest experimental point at 0.6 Å^{-1} to the value at $Q = 0$ using a maximum entropy procedure [21].

The deadtime, τ, relates the counted intensity, I_c, to the true intensity, I_0, through the formula

$$I_c = I_0 \exp(-I_0 \tau). \tag{8}$$

At HASYLAB τ was measured by varying the beam strength using iron attenuators of varying thickness in front of the sample. The known dependence of beam strength is then used to find the deadtime. More details are given in [7]. At the ESRF, τ was measured by fitting to an intensity versus slit width curve, generated by varying the width of a slit placed far from the sample [7]. This method was less accurate than that used at HASY. However, due to the large number of scans over many different beam strengths at ESRF, the ESRF data were found to be relatively insensitive to the exact value of the deadtime.

The number density of the sample is required (for example) in equation (6) for the Fourier transform. However, because no data on the isotopic variation of the bulk number density were available for methanol, we assumed that all isotopic samples had the same number density as that of CH_3OH estimated from data in the standard tables [2]. For water [7] we had found that isotopic differences in the number density affected the structural isotopic differences only a few parts in 10 000. This is much smaller than our measured structural effect in methanol or ethanol and so it is reasonable to assume that the number density differences were unimportant.

5. Results for methanol at room temperature

In figure 1 our pseudonuclear data (as given by equation (5)) for $i(Q)$ of CH_3OH (which was measured at ESRF at a temperature of 23.5 °C and at HASYLAB at 24.5 °C) are compared with the smoothed results of Narten and Habenschuss [4] for methanol at 20 °C. The ESRF line is smoother than the HASYLAB line due to the improved counting statistics in the former experiment. Both the ESRF and HASYLAB points have been rebinned in groups of four for $Q > 10$ Å^{-1}. In the region of the main peak of $i(Q)$ (near 1.7 Å^{-1}) and up to the second peak at 5.5 Å^{-1}, our measurements taken using modern synchrotron sources show much better agreement with each other than with the results of Narten and Habenschuss [4]. This is probably due partly to the much larger (≈30% as opposed to our ≈1%) multiple scattering

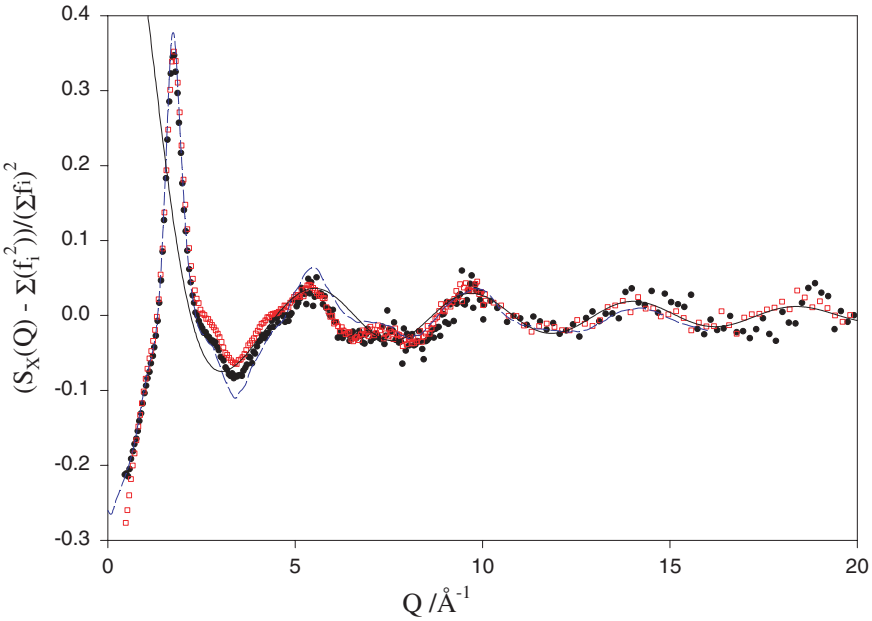

Figure 1. Pseudonuclear $i(Q)$ for methanol (CH_3OH) derived from the electronic $S_X(Q)$ using equation (5). The HASYLAB results (closed circles) are compared to the ESRF results (open squares) and literature [4] results (dashed curve). The HASYLAB and ESRF results are have been rebinned in groups of four for $Q > 10$ Å^{-1}. The data are also compared with the IAA model (solid curve) with a fitted value for r_{CO} from table 3.

Table 3. C–O distances in methanol isotopes.

Isotope	Measured r_{CO} using $Q > 10$ Å^{-1}
CH_3OH	1.450 ± 0.005 Å
CD_3OD	1.433 ± 0.005 Å
CD_3OH	1.442 ± 0.005 Å
CH_3OD	1.429 ± 0.005 Å

corrections required in the work of Narten and Habenschuss, and partly due to the fact that the results from [4] were taken at 20 °C whereas our results were acquired at $T \approx 25$ °C.

Initially, the ESRF results for $i(Q)$ did not oscillate exactly about zero as expected. Therefore, a second-order polynomial was fitted to them and adjusted to eliminate this small systematic error. This correction caused an initial difference of about 5% between the HASYLAB and ESRF principal peak heights and smaller differences elsewhere to disappear. The correction was the same for all isotopes and therefore does not appear in the isotopic differences. After correction, agreement of the $i(Q)$ curves measured at ESRF and HASYLAB is good for 0.5 Å^{-1} $< Q <$ 2.5 Å^{-1} and for $Q >$ 5 Å^{-1}. The final ESRF and HASYLAB results disagree slightly over the 2.5 Å^{-1} $> Q >$ 5.0 Å^{-1} range. Interestingly, in figure 1 both of our results disagree somewhat with the results of Narten and Habenschuss [4] over the region 3–7 Å^{-1}. However, our primary interest lies in the isotopic differences between samples measured in the same way on the same instrument, and we do not expect the above effects to alter these differences significantly.

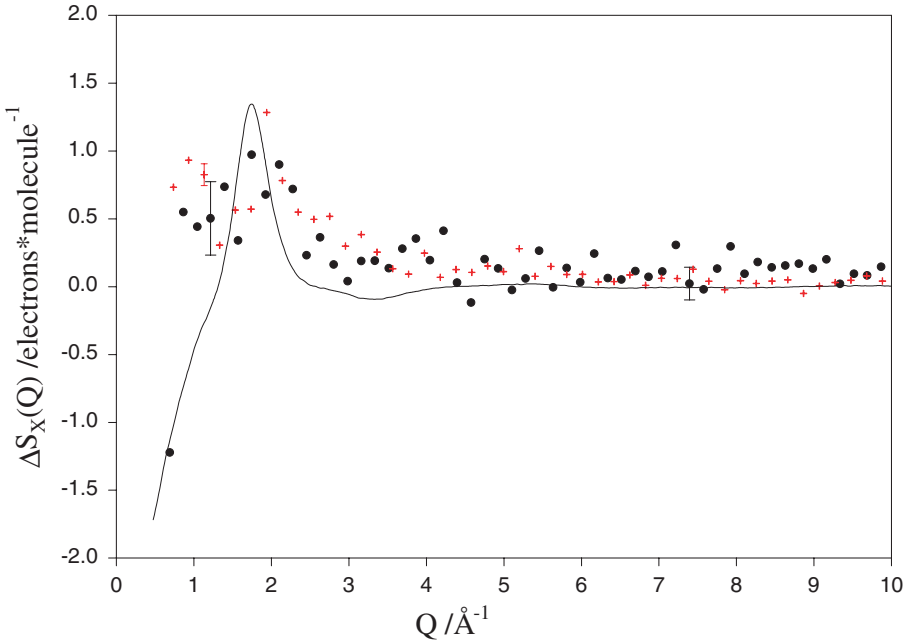

Figure 2. The isotopic difference CD_3OD–CH_3OH measured at HASYLAB at 24.5 °C (closed circles) is compared with the same difference measured at ESRF at 23.5 °C (crosses). These two isotopic differences have been rebinned in groups of four points. A scaled plot of the structure factor, $(S_X(Q) - \Sigma f_i^2)/50$ for CH_3OH measured at ESRF at 23.5 °C (solid curve) indicates that the relative size of the peak isotopic effect is about 2–3% of the total structure.

The measurement of $\Delta S_x(Q)$ for four isotopes of methanol allowed six differences to be constructed. These can be grouped into three distinct groups, each of which contains two difference measurements of a similar type: (1) double substitution, (a) CD_3OD–CH_3OH and (b) CH_3OD–CD_3OH; (2) methyl group substitution, (a) CD_3OH–CH_3OH and (b) CD_3OD–CH_3OD; and (3) hydroxyl group substitution, (a) CH_3OD–CH_3OH and (b) CD_3OD–CD_3OH. Substitutions (a) and (b) of type (2) and (3) are expected to be the same to first order, whereas those in group (1) are not the same because (1a) has both substitutions going from H to D whereas in (1b) the methyl group changes from H to D but the hydroxyl group changes from D to H.

In figure 2 the 24.5 °C results for CD_3OD–CH_3OH from ESRF and HASYLAB are compared (case 1a). These data have been smoothed by averaging over groups of four data points. The synchrotron isotopic differences clearly agree with each other, and therefore the ESRF data, which has better statistics, will be used for the room temperature differences in later figures. A scaled plot of the structure factor for methanol, $(S_X(Q)-\Sigma f_i^2)/50$, is included to show the size of the isotopic effect relative to the total structure. Since these are roughly the same size we conclude that, in Q space, isotopic effects are about 2% of the total structure factor.

The synchrotron results of figure 2 disagree with the published results (for CD_3OD–CH_3OH) of Benmore and Egelstaff [1] over the range 1–2 $Å^{-1}$ as may be seen by comparing the data in figures 2 and 3. The data in [1] were obtained using an ^{241}Am-sourced gamma ray diffractometer with long counting times. In figure 3 we compare Benmore and Egelstaff's maximum entropy smoothed results with our measurements using a natural methanol sample

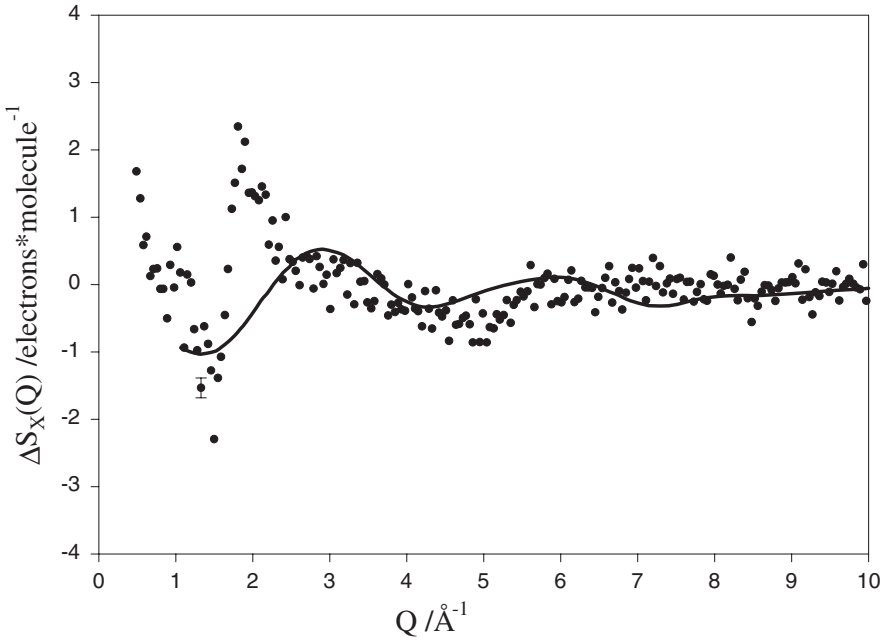

Figure 3. The difference between a pure CD_3OD sample and a CH_3OH sample contaminated with 1% by weight of water (closed circles) is compared with the CD_3OD–CH_3OH difference measured with a ^{241}Am γ source and smoothed by Benmore and Egelstaff [1] (solid curve).

containing 1% by weight of water, which is the most likely contaminant. The shape of the water-contaminated isotopic differences shown in figure 3 does not agree with the shape of the pure isotopic differences in figure 2 over the range 1–5 $Å^{-1}$ since it has an inverted and stronger peak at 1.75 $Å^{-1}$. However, the shape of the water-contaminated curve is closer to the data of Benmore and Egelstaff than the uncontaminated isotopic difference, which indicates that the Benmore and Egelstaff results may possibly have been contaminated by water. The discrepancy over 1.8–2.2 $Å^{-1}$ between the two sets of data in figure 3 could perhaps be due to differences between the amounts of water in the samples shown in the figure: for example, a lower percentage ($\sim$0.3%) for [1].

The uppermost curves, marked (a), in figure 4 show the room temperature differences measured at ESRF for CH_3OD–CH_3OH and CD_3OD–CD_3OH, which are compared with their respective maximum entropy smoothed curves (which were forced to zero in the limit at $Q = 0$). The error bars in figure 4 have been omitted for clarity: however, they are of the same size as shown in figure 2 for these differences. It is evident that the two possible ways of constructing a hydroxyl substitution effect are nearly the same to within the error bars.

In the middle curves of figure 4, marked (b), the room temperature differences measured at ESRF for CD_3OH–CH_3OH and CD_3OD–CH_3OD are shown and compared with their respective maximum entropy smoothed curves. This figure shows that the two possible ways of constructing a methyl substitution effect from our measurements yield effects of the same general shape and magnitude. Differences between the curves are on the order of 0.3 electrons per molecule, which is only about twice the size of the error bars on the ESRF measurements. The level of consistency in figure 4 is indicative of the good overall quality of our results.

Comparison of the curves in figure 4(a) and (b) shows that the methyl and hydroxyl substitution effects are very nearly the opposite of one another at room temperature. This is

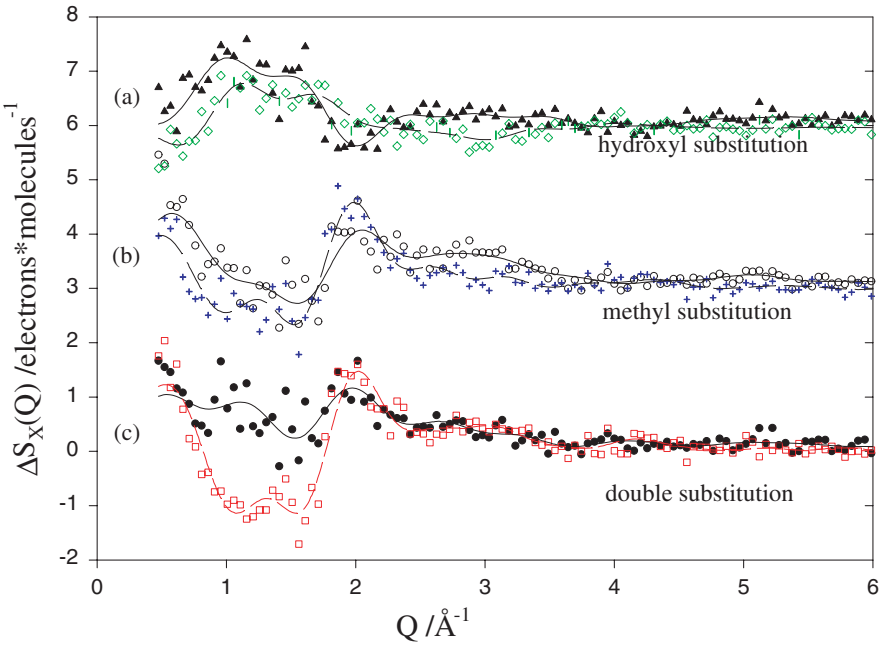

Figure 4. Several isotopic differences for methanol at $T = 23.5\,^{\circ}$C measured in 1998 at ESRF are compared with each other and with the results of maximum entropy fitting. (a) Hydroxyl substitutions (shifted by +6 electrons/molecule): the difference CH_3OD–CH_3OH (triangles) is compared with CD_3OD–CD_3OH (diamonds). Maximum entropy fits are also shown for CH_3OD–CH_3OH (solid curve) and CD_3OD–CD_3OH (dashed curve). (b) Methyl substitutions (shifted by +3 electrons/molecule): the difference CD_3OH–CH_3OH (open circles) is compared with CD_3OD–CH_3OD (crosses). Maximum entropy fits are also shown for CD_3OH–CH_3OH (solid curve) and CD_3OD–CH_3OD (dashed curve). (c) Double substitutions (unshifted): the difference CD_3OD–CH_3OH (closed circles) is compared with CD_3OH–CH_3OD (open squares). Maximum entropy fits are also shown for CD_3OD–CH_3OH (solid curve) and CD_3OH–CH_3OD (dashed curve).

most apparent where $0.5\ \text{Å}^{-1} \leqslant Q \leqslant 2.5\ \text{Å}^{-1}$ and is caused by the H methyl scattering being more intense than the D methyl scattering in 4(b), while the D hydroxyl is more intense than the H hydroxyl in 4(a).

The lower curves in figure 4, marked (c), show the room temperature differences measured at ESRF for CD_3OD–CH_3OH and CD_3OH–CH_3OD and they are compared with their respective maximum entropy smoothed curves. These two differences produce differing results because they represent the two ways of substituting at both sites. In the former difference both the hydroxyl and the methyl sites vary from D to H. In the latter difference only the methyl site varies from D to H while the hydroxyl is varied from H to D. Because the hydroxyl and methyl effects have opposite signs in the 1–2 Å^{-1} region, the latter difference results in the largest quantum effect. For all the data of figure 4 we note that the major effects occur near the principal peak of figure 1 at 1.7 Å^{-1} and at lower Q values. A previous publication has shown that the methyl and hydroxyl substitution effects of figures 4(a) and (b) may be added to yield the total effects shown in 4(c) [11].

The parameters shown in table 1 can also be obtained (using equation (4)) from the high-Q ($Q > 10\ \text{Å}^{-1}$) portions of our data for each isotope (CH_3OH shown in figure 1) to yield new estimates of these intramolecular quantities. For this purpose a least-squares fit, involving only the ESRF room temperature data, was performed by varying the carbon–oxygen intramolecular distance, (r_{CO} in equation (4)) for each isotope. The results summarized in table 3 are from [11].

A plot of the results for CH_3OH, showing the excellent agreement at high Q between the IAA model using the fitted r_{CO} and the experimental data, is included in figure 1. If the literature value for r_{CO} is used in the IAA model, the curves shifts slightly out of phase. For example, the curve shown in figure 1 crosses the x-axis at $Q = 15.2$ Å while for the literature value the curve for r_{CO} would cross the x-axis at $Q = 15.4$ Å. The values of r_{CO} from [4] may have artificially small error bars because the fitting to obtain r_{CO} was performed on smoothed data. In contrast, our fit was performed on the unsmoothed $S_X(Q)$, and if one uses more reasonable error bars (e.g. of twice the size in [4]), then there is agreement between the two CH_3OH r_{CO} measurements.

From table 3 we conclude that a single substitution of a hydrogen with a deuterium at hydroxyl site causes r_{CO} to shorten by an average of 0.015 Å. A triple substitution at a methyl site has an effect that lengthens r_{CO} by an average of 0.006 Å, which is about the same size as the error of ± 0.005 Å in the r_{CO} measurement.

6. Results for methanol at low temperatures

Five of the six isotopic differences previously shown in figure 4 for $T = 23.5\,^{\circ}$C are also shown in figure 5 for a lower temperature of $-80\,^{\circ}$C. These measurements were taken at HASYLAB over two experimental periods in 1999 and 2000. Due to a shortage of time, the CD_3OD– CH_3OD difference was not measured at $-80\,^{\circ}$C. In figure 5(a) the hydroxyl differences measured in 1999 (case 3a) and 2000 (case 3b) are compared. The plots of figure 5(b) show the excellent agreement between the 1999 and 2000 measurements of the same (case 2a: CD_3OH–CH_3OH) difference. The crosses for $Q < 0.75$ Å^{-1} were deleted (in the 1999 results) since the incident beam entered the detector at low angles and affected those data. Thus figure 5(b) confirms that differences measured during different experiments may be used in our comparisons.

The hydroxyl substitution effect on structure (figures 4(a) and 5(a)) is of about the same magnitude at both -80 and $25\,^{\circ}$C. However, the effect of D to H substitution is predominantly negative for $Q < 2$ Å^{-1} at $-80\,^{\circ}$C and positive at $25\,^{\circ}$C. That is, the hydroxyl effect has switched signs in going from the high temperature to the low temperature. For example, if the CD_3OD–CD_3OH $-80\,^{\circ}$C plot is inverted, the features in $\Delta S_X(Q)$ are in similar locations in Q-space as for the CD_3OD–CD_3OH $24.5\,^{\circ}$C plot. By comparison of figure 4(b) and 5(b), we see that the methyl substitution effect at 2 Å^{-1} is about twice as large at $-80\,^{\circ}$C as at room temperature and about four times as large at 0.5 Å^{-1}. The plots 5(a) and (b) show that the triple H substitution in methyl is about three times as large as the hydroxyl substitution. Therefore at this temperature the effect per substituted H is approximately the same for methyl and hydroxyl substitution. This is in contrast to the room temperature results of figure 4 where the single hydroxyl substitution produced a structural effect of approximately equal magnitude to triple substitution on the methyl sites.

The results at $T = -80\,^{\circ}$C show the same trend as the room temperature results in that the two ways of constructing a given difference with the measured isotopes appear to be approximately equal. As observed in the room temperature differences, the $-80\,^{\circ}$C difference results are additive. An important difference with respect to room temperature results is that at cold temperatures the effect of the hydroxyl substitutions and the methyl substitution are both negative in the 1–2 Å^{-1} range. Another difference is that the effect of double substitution is clearly dominated by the methyl effect.

Further understanding of the significance of these changes may be gained by studying the Fourier transforms to r-space of these curves, which will be presented in paper II. It may be anticipated that the intramolecular effects will be seen more clearly in r-space.

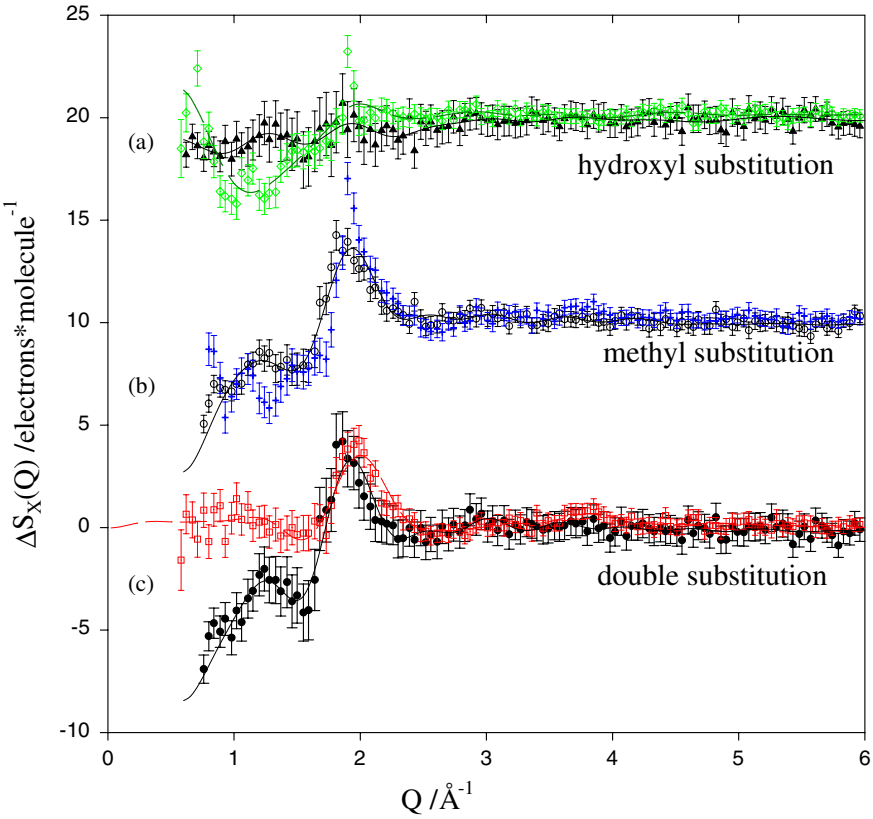

Figure 5. Several isotopic differences for methanol at $T = -80\,^{\circ}$C measured at HASYLAB are compared with each other and with the results of maximum entropy fitting. (a) Hydroxyl substitutions (shifted by +20 electrons/molecule): the difference CH_3OD–CH_3OH measured in 1999 (open diamonds) is compared with CD_3OD–CD_3OH (triangles) measured in 2000. Maximum entropy fits are also shown for CH_3OD–CH_3OH (dashed curve) and CD_3OD–CD_3OH (solid curve). (b) Methyl substitutions (shifted by +10 electrons/molecule): the difference CD_3OH–CH_3OH measured in 2000 (open circles) is compared with the same difference measured in 1999 (crosses). A maximum entropy fit is also shown for the 2000 results (solid curve). (c) Double substitutions (unshifted): the difference CD_3OD–CH_3OH (closed circles) is compared with CH_3OD–CD_3OH (open squares). Maximum entropy fits are also shown for CD_3OD–CH_3OH (solid curve) and CH_3OD–CD_3OH (dashed curve).

In figure 6 the hydroxyl substitution effect (CD_3OD–CD_3OH) at $-30\,^{\circ}$C is compared with the temperature derivative between the 24.5 °C and the $-30\,^{\circ}$C data for CD_3OH. The temperature difference (divided by 10) shows excellent agreement with the $-30\,^{\circ}$C hydroxyl substitution results. This means that substituting a single deuterium with a hydrogen at the hydroxyl position causes a structure change corresponding to a 5.5 °C decrease in temperature. We observed that the excellent agreement in figure 6 using the CD_3OH temperature difference worked equally well when the CD_3OD temperature difference was used.

In figure 7 the double substitution effect in CD_3OD–CH_3OH at $-80\,^{\circ}$C is compared with the difference in $S_X(Q)$ for CH_3OH at temperatures of -80 and 24.5 °C. The temperature difference in $S_X(Q)$ (divided by 3) shows excellent agreement with the $-80\,^{\circ}$C double substitution results. This means that substituting all the deuterium in CD_3OD with hydrogen causes a structure change corresponding to (approximately) a 35 °C increase in temperature

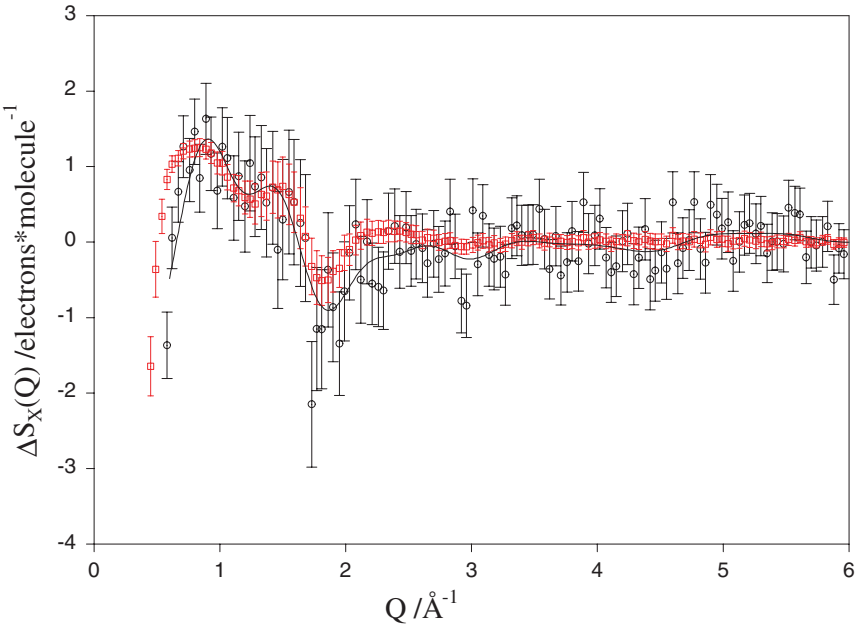

Figure 6. The isotopic differences CD_3OD–CD_3OH at $T = -30\,^{\circ}C$ (open circles) are compared with a temperature difference for CD_3OH $\{T = 24.5\,^{\circ}C\}$–$\{T = -30\,^{\circ}C\}$ divided by 10 (open squares) and with the maximum entropy fit to them (solid curve). These results were measured at HASYLAB.

Table 4. Effective temperature change (°C) caused by deuteration in methanol.

Temperature	Triple substitution at methyl site	Substitution at hydroxyl site
24.5	-5.5 ± 1	$+4 \pm 1$
-30		5.5 ± 1
-80	-35 ± 8	-6.5 ± 1

about the mean temperature, $T = -28\,^{\circ}C$. Once again the excellent agreement in figure 7 using the CH_3OH temperature difference worked equally well when the CD_3OD temperature difference was used. The effect of deuteration at $T = -80\,^{\circ}C$ is analogous to cooling (in this case by 35 °C), as might be expected for the heavier deuterium atom.

The isotopic differences shown in figures 4 and 5 can be compared with the temperature difference results and the measured temperature difference can be scaled to produce an effective temperature change between two different isotopic samples. The results of such a process (averaged for the two ways of producing a methyl or hydroxyl difference) are shown as a function of temperature in table 4. The errors shown in table 4 were estimated by varying a factor scaling the temperature until the smoothed isotopic difference fell outside of the error bars of the temperature difference.

The results of table 4 show that it is possible for heavier isotopes (with reduced librational motions) to actually have a structure similar to that of a lighter isotope measured at a higher temperature. This heating effect is difficult to understand in simple terms. However, Prigogine [22] has suggested that heating effects due to deuteration could be caused by reduced molecular polarizability (and hence reduced van der Waals attractive forces) in the heavier isotope.

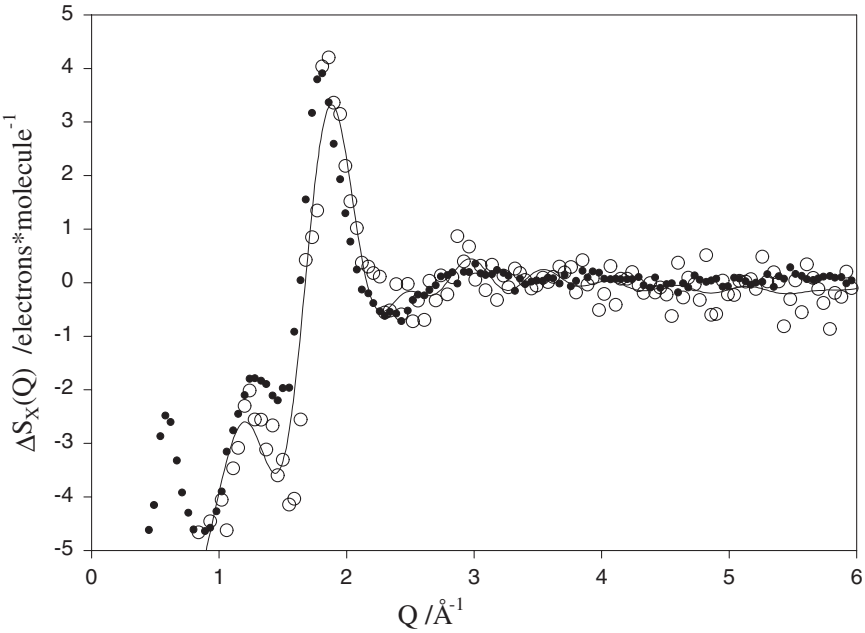

Figure 7. The isotopic differences CD_3OD–CH_3OH at $T = -80\,^{\circ}C$ (open circles) are compared with one-third of the temperature difference for CH_3OH $\{T = -80\,^{\circ}C\}$–$\{T = 24.5\,^{\circ}C\}$ (closed circles) and with the results of their maximum entropy fit (solid curve). All these experimental results were measured at HASYLAB.

It would be very interesting to measure more accurate partial structure factors (by the technique of isotopic contrast neutron diffraction) using different temperatures for different isotopic samples (chosen using data such as that presented in table 4).

7. Conclusions

These experiments have shown clearly measurable influences upon liquid structure caused by the structural quantum effects in methanol, which vary with temperature and molecular group. They set clear limits on the accuracy of the standard H/D substitution method for the analysis of neutron diffraction data in terms of partial structure factors for methanol. They have also indicated how those experiments might be improved by using the different temperatures quoted above (table 4) for their different isotopic measurements.

Because of the advantages of the high-intensity and high-energy radiation from synchrotron sources that is available today, our static electronic structure factors for CH_3OH required smaller attentuation and multiple scattering corrections than older results (e.g. [4]). Consequently, there appear to be reproducible differences between our experiments and some of the older results. Our new results will be highly suitable for comparison with future structure determinations.

The isotopic differences showed a high degree of reproducibility between different experiments, and in the two different ways a given difference could be constructed from the four isotopes studied.

At room temperature, the effect of a single substitution at the hydroxyl site has been shown to have an effect of a similar magnitude and shape but opposing sign to that of the triple

substitution at the methyl site. This indicates the importance of hydrogen bonding in these liquids at room temperature and the relative importance of the hydroxyl site in the intra- and intermolecular structure of these compounds.

A careful analysis of figures 4–7 and table 4 shows that the isotopic structural difference corresponds to a single temperature shift with a magnitude and sign that varies as a function of substitution site and temperature. For example, the substitution of a hydrogen with a deuterium at the hydroxyl site at $-30\,^{\circ}$C has been shown to correspond to heating methanol by $5.5\,^{\circ}$C in figure 6. The scale of the temperature derivative was chosen to mimic the hydroxyl effect. Though not shown, a temperature shift of opposing sign would be very similar to the effect of substituting deuterium for hydrogen at the methyl sites at room temperature. However, at $-80\,^{\circ}$C, a hydroxyl substitution produces a cooling effect (figure 7). Therefore, depending on the site of the substitution and the temperature, the effect of deuteronic substitution can correspond to either heating or a cooling effect. The general shape of the temperature derivative for methanol seen in figures 6 and 7 is sufficient to explain any of our measured isotopic differences if the temperature-dependent nature of the competing hydroxyl and methyl substitution effects is taken into account. The results of such an analysis of all of our measured isotopic differences for methanol was summarized in table 4. Given the approximately additive nature of the two effects [11], further data of the kind shown in table 4 could be used to generate temperature-dependent functions and so approximate the isotopic difference at a variety of temperatures for any of the methanol isotopes studied. The $\sim$20% error bars in table 4 indicate that temperature differences could be use to correct the 2% structural isotopic effects (at room temperature) to within about 0.5% for different isotopes. As more measurements are compiled the precision of this approximation can be tested in greater detail and hopefully improved.

In table 4, the effective temperature shift of the methyl H–D substitution effect is seen to correspond to cooling at room temperature which increases in magnitude with decreasing temperature. The effective temperature shift corresponding to the hydroxyl H to D substitution effect is seen to correspond to warming at room temperature and also at $-30\,^{\circ}$C. It changes sign (becoming a 'cooling' effect) as temperature is decreased to $-80\,^{\circ}$C but its magnitude changes much less than the methyl effect.

The increase of the methyl effect with decreasing temperature is consistent with the notion of this effect being dominated by isotopic differences in ground state librations. The more complicated behaviour of the structural effects of hydroxyl substitution indicates that a there are probably significant contributions due to perturbations of the hydrogen bonding structure of liquid methanol when the hydroxyl site is varied isotopically. Therefore, in the following discussion, we will refer to 'librational' and 'H-bonding' effects in comparing our results on methanol to those observed in water [7]: this is understood to be an approximation to facilitate discussion. Clearly substitution at the methyl site will have some small effect on the H-bonding and the substitution at the hydroxyl site will change the ground state librations of the methanol molecule (though presumably less so than the methyl substitution).

At room temperature, deuteronic substitution at the hydroxyl site corresponds to opposing temperature changes for water and methanol. Studies on water have shown that substitution of both hydrogens with deuterium had the same effect on $S_X(Q)$ as *cooling* by $5.5\,^{\circ}$C [7] whereas we have shown above that such a substitution produces a heating effect in methanol. This behaviour can be understood by considering the fact that in water, unlike for methanol, the librational and H-bonding effects of isotopic substitution cannot be separated. There are two possibilities. Firstly, the librational and H-bonding effects could be of the same sign in room temperature water as they were for methanol at $-80\,^{\circ}$C. At such conditions, both liquids are about $20\,^{\circ}$C above their freezing points. In methanol at these conditions, the librational effect was seen to dominate. This is a cooling effect as was observed in water. Secondly, the

librational and H-bonding effects might be competing (as in room temperature methanol), and if this is the case, the experiments on room temperature water will have shown that the isotopic difference is dominated by librational effects. Future experiments can be designed to explore the temperature shifts of each corresponding effect in water or methanol.

The unexpected results described above require a detailed interpretation based, for example, on careful quantum molecular dynamics simulations. The detailed comparison of the full isotopic differences at $-80\,^{\circ}$C with data from a $105\,^{\circ}$C temperature shift in methanol is especially interesting and justifies further study. In particular, simulation studies of these effects could show the relative importance of quantum mechanical effects in the librational motions and hydrogen bonding and explain why in some cases isotopic substitution produces a heating effect and in others a cooling effect.

It is anticipated that these observations will be useful in planning future neutron scattering isotopic substitution experiments.

Acknowledgments

Staff at the Hamburger Synchrotronstrahlungslabor HASYLAB and the European Synchrotron Radiation Facility ESRF are thanked for providing the apparatus and the beamtime, and for their assistance in conducting the experiments. Professor A K Soper is thanked for many useful discussions concerning the x-ray data. The work of the Canadian participants was supported by a grant from NSERC Canada. This work was performed in part under contract no W-31-109-ENG-38 with the US Department of Energy.

References

[1] Benmore C J and Egelstaff P A 1996 *J. Phys.: Condens. Matter* **8** 9429–32
[2] Lide D R (ed) (1998–9) *CRC Handbook of Chemistry and Physics* 79th edn
[3] Del Buono G S, Rossky P J and Schnitker J 1991 *J. Chem. Phys.* **95** 3728–37
[4] Narten A H and Habenschuss A 1984 *J. Chem. Phys.* **80** 3387
[5] Weitkamp T, Neuefeind J, Fischer H E and Zeidler M D 2000 *Mol. Phys.* **98** 125
[6] Magini M, Paschina G and Piccaluga G 1982 *J. Chem. Phys.* **77** 2051–6
[7] Tomberli B, Benmore C J, Egelstaff P A, Neuefeind J and Honkimäki V 2000 *J. Phys.: Condens. Matter* **12** 2597–616
[8] Soper A K 1984 *Chem. Phys.* **88** 187
[9] Yamaguchi T, Hidaka K and Soper A K 1999 *Mol. Phys.* **96** 1159
[10] Benmore C J and Loh Y L 2000 *J. Chem. Phys.* **112** 5877–83
[11] Tomberli B, Benmore C J, Egelstaff P A, Neuefeind J and Honkimäki V 2001 *Europhys. Lett.* **51** 341–7
[12] Guinier A 1963 *X-ray Diffraction in Crystals, Imperfect Crytsals and Amorphous Bodies* (New York: Freeman)
[13] Lovesy S W 1984 *Theory of Neutron Scattering from Condensed Matter* vol 1 (Oxford: Clarendon) ch 6
[14] Hubbell J H, Veigele W J, Briggs E A and Howerton R J 1975 *J. Phys. Chem. Ref. Data* **4** 471
[15] Montague D G, Gibson I P and Dore J C 1981 *Mol. Phys.* **44** 1355–67
[16] Lees R M and Baker J G 1968 *J. Chem. Phys.* **48** 5299
[17] Kimura K and Kubo M 1959 *J. Chem. Phys.* **30** 151–8
[18] Root J H, Egelstaff P A and Hime A 1986 *Chem. Phys.* **109** 5164
[19] Soper A K and Egelstaff P A 1980 *Nucl. Instrum. Methods* **178** 415
[20] Palman H H and Pings C J 1962 *J. Appl. Phys.* **33** 2635
[21] Soper A K, Andreani C and Nardone M 1993 *Phys. Rev.* E **47** 2598
[22] Prigogine I 1957 *The Molecular Theory of Solutions* (Amsterdam: North-Holland) ch XVIII